

SPHERICAL WAVES IN CONICAL TEM CELLS

D. Pouhè

Technical University Berlin

Dept. of High Frequency and Semi-Conductor System Tech.

Sekretariat HFT 5-1, Einsteinufer 25, 10587 Berlin, Germany

Abstract—The propagation of the TEM and higher order Modes in GTEM cells is theoretically treated in this work in spherical coordinates. The derived wave equation for the principal mode is solved analytically in two different ways. In which case, two general closed-solutions are derived. In addition to this a simple approximation for the special case of the symmetric cells is presented. For higher order waves, E- and H-modes are determined by solving the Helmholtz equations for phasor. By imposing the boundary conditions on fields, the determination of local higher-order modes is, for symmetric cells, reduced to the solution of a simple transcendental equation $L_n^{m\nu}(\cos\theta) = 0$. For asymmetric cells, the matching-points method is applied. In the longitudinal direction, the propagation of the fields is examined by means of cylindrical functions which are combined with the spherical one. Furthermore, since the GTEM cell is a conical-horn resonator, the resonance behavior of the cell is investigated. The main advantages of the method amongst others are its simplicity and high degree of accuracy. Its appeal consist of precise description of the cell's geometry compared with the other methods.

1. INTRODUCTION

A common point in most of the methods used in the analysis of electromagnetic fields in Gigahertz Transverse Electromagnetic (GTEM) cell is the approximation of the cell to a rectangular pyramidal horn. Since this approximation is an extension of a rectangular waveguide, calculation of the fields is forcibly carried on in the cartesian coordinate system [1–3]. The GTEM Cell is but, a coaxial-conicalhorn, terminated with a combination of discrete resistances and RF-absorbers, it is therefore called-for and convenient to use spherical coordinates to analyze the field distribution in the cell. Two pertinent reasons for this approach are as follows:

- 1) There is no orthogonal co-ordinate system e_1, e_2, e_3 where the plane surfaces $e_1 = const.$ and $e_2 = const.$ are identical with the walls of a conical horn.
- 2) The propagation of each mode (both TEM and Higher order waves) in a GTEM Cell depends to a large extent on the geometrical shape of the cell, although the part played by the method of the excitation responsible for its formation and form is of course not of less significance or importance.

This work investigates the propagation of spherical TEM-, TE- and TM-waves in GTEM cells. For this purpose, quasi stationary conditions are assumed for the TEM case; that is, only the principal mode propagates in the cell. The fields are obtained by solving the Laplace equation.

For higher electromagnetic waves, the cell will no longer be assumed to be infinitely long; that is, quasi stationary conditions are no longer assumed. The fields (TM- and TE-waves) are then determined by solving the Helmholtz equations for phasor fields in spherical coordinates. By imposing the boundary conditions on fields, the determination of local higher-order modes is, for symmetric cells, reduced to the solution of a simple transcendental equation $L_n^{m\nu}(\cos \vartheta) = 0$. For asymmetric cells, the matching-points method is applied. In the longitudinal direction, the propagation of the fields is examined by means of cylindrical functions which are combined with the spherical one. Furthermore, since the GTEM cell is a conical-horn resonator, the resonance behavior of the cell is investigated.

The main advantages of the method amongst others are its simplicity, high degree of accuracy. Its appeal consist of precise description of the cell's geometry compared with the other methods.

Notice that, throughout this work, the time harmonic dependence $e^{j\omega t}$ has been suppressed.

2. THE TEM MODE

2.1. Calculation of the Fields

2.1.1. The Wave Equation and Its Solutions

Let us assumed that only the principal wave i.e., the TEM-Mode propagates in the cell. We can therefore express the \mathbf{H} -field as a rotation of an r oriented potential $\mathbf{\Pi}_r$

$$\mathbf{H} = \nabla \times \mathbf{\Pi}_r. \quad (1)$$

The potential $\mathbf{\Pi}_r$ should as such satisfied the Laplace equation. For this purpose, the GTEM-cell will be implemented in spherical

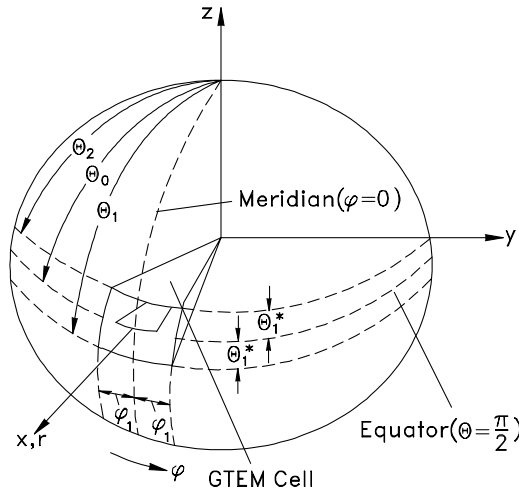


Figure 1. The GTEM-cell in spherical coordinates.

coordinates (Fig. 1) and the solutions of equation (2) will be written in this coordinate system.

$$\nabla^2 \mathbf{\Pi}_r = \frac{1}{r^2 \sin \vartheta} \cdot \left[\frac{\partial}{\partial \vartheta} \left(\sin \vartheta \cdot \frac{\partial \mathbf{\Pi}_r}{\partial \vartheta} \right) + \frac{\partial}{\partial \varphi} \cdot \left(\frac{1}{\sin \vartheta} \cdot \frac{\partial \mathbf{\Pi}_r}{\partial \varphi} \right) \right] = 0 \quad (2)$$

To solve this partial differential equation, we apply the product solution method — also called method of separation of variables. The formulation

$$\mathbf{\Pi}_r = D(\vartheta) \cdot U(\varphi) \quad (3)$$

substituted in (2) leads to equation (4)

$$\frac{1}{D(\vartheta) \sin \vartheta} \cdot \frac{\partial}{\partial \vartheta} \left(\sin \vartheta \cdot \frac{\partial D \vartheta}{\partial \vartheta} \right) + \frac{1}{U \cdot \sin^2 \vartheta} \cdot \frac{\partial^2 U}{\partial \varphi^2} = 0, \quad (4)$$

which may be separated in two ordinary independent differential equations (5), (6) since D is a function of ϑ and U is a function of φ respectively:

$$\frac{\partial^2 U(\varphi)}{\partial \varphi^2} + m^2 U(\varphi) = 0; \quad m \in \mathbf{R} \quad (5)$$

$$\frac{\partial^2 D(\vartheta)}{\partial \vartheta^2} + \cot \vartheta \cdot \frac{\partial D(\vartheta)}{\partial \vartheta} - \frac{m^2}{\sin^2 \vartheta} D(\vartheta) = 0 \quad (6)$$

The solutions of the first equation are well known. They are

$$U(\varphi) = A' \sin(m\varphi) + B' \cos(m\varphi). \quad (7)$$

In the case of φ -direction, an even solution is needed. This leads to the following simplification

$$U(\varphi) = B' \cos(m\varphi). \quad (8)$$

The second equation (6) will be solved in two different ways.

The first method: The Legendre's solution Equation (6) is an equation of Bocher's class. More precisely, it is a particular case of the general Legendre wave equation [5, 6]

$$(z^2 - 1) \frac{d^2 Z}{dz^2} + 2z \frac{dZ}{dz} + \left[\chi^2 a^2 (z^2 - 1) - p(p + 1) - \frac{m^2}{z^2 - 1} \right] \cdot Z = 0. \quad (9)$$

In fact, by substituting in (9) $\chi = p = 0$ and $D(\vartheta) = Z$, we obtain with $z = \cos \vartheta$ the equation (6). The general solution of this equation is [4-6]:

$$D(\vartheta) = A \cdot \mathcal{P}_0^m(\cos \vartheta) + B \cdot \mathcal{Q}_0^m(\cos \vartheta) \quad (10)$$

whereby

$$\mathcal{P}_0^m(z) = z \sum_{l=0}^{l=\infty} \frac{(-1)^l \cdot \Delta_l(1) \cdot z^{2l}}{(2l+1)!} \text{ and } \mathcal{Q}_0^m(z) = \sum_{l=0}^{l=\infty} \frac{(-1)^l \cdot \Delta_l(0) \cdot z^{2l}}{(2l)!}. \quad (11)$$

The determinants $\Delta_l(1)$ and $\Delta_l(0)$ in equations (11) are given by equations (12) and (13), where $B_2 = -m^2$ and $B_{2k} = -k \cdot m^2$ with $k > 1$.

\mathcal{P}_0^m and \mathcal{Q}_0^m are the general Legendre wave functions of the zero order, where \mathcal{P}_0^m and \mathcal{Q}_0^m are of the first and second kind respectively. These general Legendre functions are not to be confused with the associated functions P_n^m and Q_n^m nor with the familiar Legendre polynomes P_n and Q_n . The last two arts of functions can be derived from the general one. More details about this functions are reported in the literature [4, 5]. Combining (7) and (8) under consideration of the boundary conditions, the potential is completely determined. But before going on with the investigation of the final expression of $\mathbf{\Pi}_r$, let us examine the second solution.

The second method: The alternative solution We would like to propose an alternative solution of equation (6) in this section. This

solution is based on the method of variation of constants.

$$\Delta_l(1) = \left| \begin{array}{cccccc} B_2 - 2 & 2 \cdot 3 & 0 & 0 & \dots & 0 \\ B_4 - 2 & B_2 - 6 & 4 \cdot 5 & 0 & \dots & 0 \\ B_6 - 2 & B_4 - 6 & B_2 - 10 & 6 \cdot 7 & 0 & \dots & 0 \\ \dots & \dots & \dots & \dots & \dots & \dots & \dots \\ B_{2l-2} - 2 & B_{2l-4} - 6 & B_{2l-6} - 10 & \dots & \dots & (2l-2)(2l-1) \\ B_{2l} - 2 & B_{2l-2} - 6 & B_{2l-4} - 10 & \dots & \dots & B_2 - 4l + 2 \end{array} \right| \quad (12)$$

and

$$\Delta_l(0) = \left| \begin{array}{cccccc} B_2 & 1 \cdot 2 & 0 & 0 & \dots & 0 \\ B_4 & B_2 - 4 & 3 \cdot 4 & 0 & \dots & 0 \\ B_6 & B_4 - 4 & B_2 - 8 & 5 \cdot 6 & 0 & \dots & 0 \\ \dots & \dots & \dots & \dots & \dots & \dots & \dots \\ B_{2l-2} & B_{2l-4} - 4 & B_{2l-6} - 8 & \dots & \dots & \dots & (2l-3)(2l-2) \\ B_{2l} & B_{2l-2} - 4 & B_{2l-4} - 8 & \dots & \dots & \dots & B_2 - 4(l-1) \end{array} \right| \quad (13)$$

The multiplication of equation (6) with $\sin \vartheta$ and its subsequent division with $D(\vartheta)$ leads to the nonhomogeneous linear differential equation of the second order (14):

$$\begin{aligned} \frac{1}{\sin \vartheta} \cdot \frac{\partial}{\partial \vartheta} \left(\sin \vartheta \cdot \frac{\partial D(\vartheta)}{\partial \vartheta} \right) - \frac{m^2}{\sin^2 \vartheta} \cdot D(\vartheta) &= 0 \\ \Leftrightarrow \frac{\frac{\partial}{\partial \vartheta} \left[\sin \vartheta \cdot \frac{\partial D(\vartheta)}{\partial \vartheta} \right]}{D(\vartheta)} - \frac{m^2}{\sin \vartheta} &= 0. \end{aligned} \quad (14)$$

Let $a(\vartheta) = \sin \vartheta$, and $f(\vartheta) = \frac{m^2}{\sin \vartheta}$. By substituting these terms in (14), we have

$$\frac{\frac{\partial}{\partial \vartheta} [a(\vartheta) \cdot D'(\vartheta)]}{D(\vartheta)} = f(\vartheta). \quad (15)$$

Equation (15) is an inhomogeneous differential equation of second order. Let us first solve the *homogeneous equation* (16):

$$\frac{\partial}{\partial \vartheta} [a(\vartheta) \cdot D'(\vartheta)] = 0. \quad (16)$$

This equation can also be rewritten as

$$\begin{aligned} \frac{\partial [a(\vartheta) \cdot D'(\vartheta)]}{\partial \vartheta} = 0 &\iff a'(\vartheta) \cdot D'(\vartheta) + a(\vartheta) \cdot D''(\vartheta) = 0 \\ &\iff \frac{a'(\vartheta)}{a(\vartheta)} + \frac{D''(\vartheta)}{D'(\vartheta)} = 0. \end{aligned} \quad (17)$$

Integrating (17) yields

$$\begin{aligned} \ln(D'(\vartheta)) &= -\ln(a(\vartheta)) + k, \quad \text{where } k = \ln(k_0), \quad k_0 \text{ is a constant} \\ &\iff \ln\left(\frac{D'(\vartheta)}{k_0}\right) = \ln(a^{-1}(\vartheta)) \\ &\implies D'(\vartheta) = k_1 \cdot \frac{1}{a(\vartheta)} = \frac{k_1}{\sin \vartheta}. \end{aligned} \quad (18)$$

Since we need to determine $D(\vartheta)$ and not $D'(\vartheta)$, equation (18) has to be integrated with respect to ϑ . We then have

$$D(\vartheta) = \int \frac{k_1}{\sin \vartheta} d\vartheta = k_1 \cdot \ln \left| \tan \frac{\vartheta}{2} \right| + k_2. \quad (19)$$

$D(\vartheta)$ is the general solution of the homogeneous differential equation (16).

The general solution of equation (15) is obtained by making use of the well-known method of variation of constants [8]. This requires that: $D(\vartheta)$ be a solution of the *nonhomogeneous equation* (15) when and only when k_1 and k_2 as functions of ϑ are solutions of the set of equations (20).

$$\begin{aligned} k'_1 \cdot \ln \left| \tan \frac{\vartheta}{2} \right| + k'_2 &= 0 & (a) \\ k'_1 \left(\frac{1}{\tan \frac{\vartheta}{2}} \cdot \frac{1}{\cos^2 \frac{\vartheta}{2}} \right) &= \frac{m^2}{\sin \vartheta} & (b) \end{aligned} \quad (20)$$

The solution of eq. (20b)

$$k_1 = \frac{1}{2} m^2 \vartheta + c_1. \quad (21)$$

is obtained after transformation with the aid of the addition theorem of trigonometric functions and integration with respect to ϑ . In (21) c_1 is a constant of integration. Equation (20a) leads therefore to

$$k'_2 = -k'_1 \cdot \ln \left| \tan \frac{\vartheta}{2} \right| = -\frac{1}{2}m^2 \ln \left| \tan \frac{\vartheta}{2} \right| \tag{22}$$

and, by integrating k'_2 with respect to ϑ we have [7]:

$$k_2 = -m^2 \left[\frac{\vartheta}{2} \ln \frac{\vartheta}{2} - \frac{\vartheta}{2} + \sum_{n=1}^{\infty} \frac{2^{2n}(2^{2n-1} - 1)B_n}{n(2n + 1)!} \cdot \left(\frac{\vartheta}{2}\right)^{2n+1} + c_2 \right], \tag{23}$$

whereby c_2 is a constant of integration and

$$B_n = \frac{(2n)!}{2^{2n-1} \cdot \pi^{2n}} \sum_{l=1}^{\infty} \frac{1}{l^{2n}} \tag{24}$$

are the Bernoulli's numbers [9].

The general solution $D(\vartheta)$ of the inhomogeneous equation (15) is obtained from (19) and is [10]:

$$D(\vartheta) = \frac{1}{2}m^2\vartheta \left(\ln \left| \frac{\tan \frac{\vartheta}{2}}{\frac{\vartheta}{2}} + 1 \right| \right) - m^2 \sum_{n=1}^{\infty} \frac{2^{2n}(2^{2n-1} - 1)B_n}{n(2n + 1)!} \left(\frac{\vartheta}{2}\right)^{2n+1} + c_1 \ln \left| \tan \frac{\vartheta}{2} \right| - m^2 \cdot c_2. \tag{25}$$

c_1 and c_2 are constants which have to be determined according to the boundary conditions. The B_n as defined above, are the Bernoulli's numbers.

Again, the potential and therefore the field components are completely determined by combining (7) and (25) under consideration of the boundary conditions. This last point is the focus of the next section.

2.1.2. The Complete Determination of the Potential and Fields

For a complete determination of the potential and subsequently, the fields, the boundary conditions on the surrounding metal walls, on the inner conductor as well as in the gap regions between the septum's end and the outer metal walls must be satisfied.

There are five conductors, whereby the four outer ones are at the same zero-potential and the center conductor having a V_o voltage. This means that in ϑ direction at $\vartheta = \vartheta_1$ and $\vartheta = \vartheta_2$ as well as in the φ -direction at $\varphi = \pm\varphi_1$ the potential vanishes. The boundaries in the azimuthal direction require that $U(\pm\varphi_1) = 0$ i.e.,

$$\cos(m\varphi_1) = 0 \implies m_n = \frac{(2n - 1)}{\varphi_1} \cdot \frac{\pi}{2}, \tag{26}$$

with $n = 1, 2, 3, \dots$

Hence, the numbers m_n are determined and with them the function

$$U_{m_n}(\varphi) = B'_{m_n} \cdot \cos(m_n\varphi). \tag{27}$$

In order to satisfy the boundary conditions in ϑ direction, the cell is subdivided in two regions (1) and (2) at the plane $\vartheta = \vartheta_0$ where the septum is placed (Fig. 2). (1) denotes the lower region and (2) indicates the upper one. ϑ_1 and ϑ_2 are therefore the lower and upper values of ϑ at the boundaries respectively. Along the planes $\vartheta = \vartheta_1$ and $\vartheta = \vartheta_2$ we have:

$$\begin{aligned} A_{m_n}^{(1,2)} \cdot \mathcal{P}_0^{m_n}(\cos \vartheta_{1,2}) + B_{m_n}^{(1,2)} \cdot \mathcal{Q}_0^{m_n}(\cos \vartheta_{1,2}) &= 0. \\ \implies B_{m_n}^{(1,2)} &= -A_{m_n}^{(1,2)} \cdot \frac{\mathcal{P}_0^{m_n}(\cos \vartheta_{1,2})}{\mathcal{Q}_0^{m_n}(\cos \vartheta_{1,2})} \end{aligned} \tag{28}$$

In general, the function $D_{m_n}^{(1,2)}$ becomes

$$\begin{aligned} D_{m_n}^{(1,2)}(\vartheta) &= \\ \frac{A_{m_n}^{(1,2)} \cdot [\mathcal{Q}_0^{m_n}(\cos \vartheta_{1,2}) \cdot \mathcal{P}_0^{m_n}(\cos \vartheta) - \mathcal{P}_0^{m_n}(\cos \vartheta_{1,2}) \cdot \mathcal{Q}_0^{m_n}(\cos \vartheta)]}{\mathcal{Q}_0^{m_n}(\cos \vartheta_{1,2})}. \end{aligned} \tag{29}$$

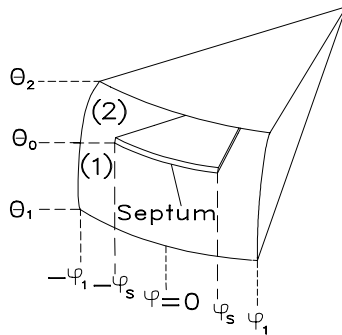


Figure 2. The calculated model.

Thus the last function for the description of the potential is completely determined. By virtue of (3), we have the following resulting potential $\Pi_{(1,2)r}$ in which the product, $B'_{m_n} \cdot A_{m_n}^{(1,2)}$, is denoted as a single new constant $C_{m_n}^{(1,2)}$:

$$\Pi_r^{(1,2)}(\varphi, \vartheta) = \sum_{n=1}^{\infty} C_{m_n}^{(1,2)} \cdot \mathcal{S}_{0,(1,2)}^{m_n}(\cos \vartheta) \cos(m_n \varphi) \quad (30)$$

where

$$\begin{aligned} \mathcal{S}_{m_n}^{(1,2)}(\cos \vartheta) = \\ \frac{\mathcal{Q}_0^{m_n}(\cos \vartheta_{1,2}) \cdot \mathcal{P}_0^{m_n}(\cos \vartheta) - \mathcal{P}_0^{m_n}(\cos \vartheta_{1,2}) \cdot \mathcal{Q}_0^{m_n}(\cos \vartheta)}{\mathcal{Q}_0^{m_n}(\cos \vartheta_{1,2})} \cdot \cos(m_n \varphi). \end{aligned} \quad (31)$$

In equations (28) to (30), the indices m_n are defined as stated above. The subscripts 1 and 2 denote the regions below and above the inner conductor, respectively. With equation (30), the potential in both regions are up to the integration's constants $C_{1,m_n}^{(1)}$ and $C_{2,m_n}^{(2)}$ completely determined. The determination of this last terms is dictated by the continuity limit conditions between regions (1) and (2) at the plane $\vartheta = \vartheta_0$ in the gape regions between the end of the septum and the metal walls and, the value of the potential on the inner conductor as well.

On the inner conductor, we impose the potential level of $V_o = 1V$, which means requiring, respectively, the following

$$\Pi_r^{(1)}(\varphi, \vartheta_0) = 1, \quad \text{and} \quad \Pi_r^{(2)}(\varphi, \vartheta_0) = 1 \quad \text{for} \quad -\varphi_s \leq \varphi \leq \varphi_s. \quad (32)$$

that is

$$\begin{aligned} \sum_{n=1}^{\infty} C_{m_n}^{(1)} \cdot \mathcal{S}_1^{m_n}(\cos \vartheta_0) \cos(m_n \varphi) &= 1 \quad \text{and} \\ \sum_{n=1}^{\infty} C_{m_n}^{(2)} \cdot \mathcal{S}_2^{m_n}(\cos \vartheta_0) \cos(m_n \varphi) &= 1 \end{aligned} \quad (33)$$

both for $-\varphi_s \leq \varphi \leq \varphi_s$

In the gap regions, we require the continuity of the potential meaning that

$$\Pi_r^{(1)}(\varphi, \vartheta_0) = \Pi_r^{(2)}(\varphi, \vartheta_0) \quad \text{for} \quad -\varphi_1 < \varphi < -\varphi_s \quad \text{and} \quad \varphi_s < \varphi < \varphi_1, \quad (34)$$

that is

$$\sum_{n=1}^{\infty} C_{m_n}^{(1)} \cdot \mathcal{S}_1^{m_n}(\cos \vartheta_0) \cos(m_n \varphi) = \sum_{n=1}^{\infty} C_{m_n}^{(2)} \cdot \mathcal{S}_2^{m_n}(\cos \vartheta_0) \cos(m_n \varphi)$$

for $-\varphi_1 < \varphi < -\varphi_s$ and $\varphi_s < \varphi < \varphi_1$ (35)

The unknown coefficients $C_{m_n}^{(1)}$ and $C_{m_n}^{(2)}$ for the potential distribution in the cell can now be obtained numerically from the set of equations (33) and (35) with the aid of the point-matching method. In the above equations, $-\varphi_s$ and $+\varphi_s$ are the left and right values of φ at the septum's end respectively (Fig. 2).

In our investigations in this part of the work up till now, we only considered the first solution presented above. However, the derivation of a closed-form formula of the potential in both regions can be carried out in a similar way to the previous treatment out going from the proposed second solution. Consequently we will restrict attention in the following paragraph to expressions of the potential derived using the second method and write down the answers directly. In this case the potential is given by

$$\begin{aligned} \mathbf{\Pi}_r^{(1,2)}(\vartheta, \phi) = & \sum_{n=1}^{\infty} \left\{ A_{m_n}^{(1,2)} \left\{ \frac{1}{2} m_n^2 \left[\vartheta \left(\ln \left| \frac{\tan \frac{\vartheta}{2}}{\frac{\vartheta}{2}} \right| + 1 \right) \right. \right. \right. \\ & - \vartheta_{1,2} \left(\ln \left| \frac{\tan \frac{\vartheta_{1,2}}{2}}{\frac{\vartheta_{1,2}}{2}} \right| + 1 \right) + \sum_{k=1}^{\infty} \frac{2^{2k+1} (2^{2k-1} - 1) B_k}{k(2k+1)!} \\ & \left. \left. \left. \cdot \left[\left(\frac{\vartheta_{1,2}}{2} \right)^{2k+1} - \left(\frac{\vartheta}{2} \right)^{2k+1} \right] \right] \right\} + C_{m_n}^{(1,2)} \ln \left| \frac{\tan \frac{\vartheta}{2}}{\tan \frac{\vartheta_{1,2}}{2}} \right| \right\} \\ & \cdot \cos(m_n \phi), \end{aligned} \tag{36}$$

where $A_{m_n}^{(1,2)}$, $C_{m_n}^{(1,2)}$ are unknown constants of integration, which have to be determined according to the boundary conditions and following the procedure described above. We recalled that the subscript 1 and 2 denote the lower and upper regions as stated above.

The magnetic field components H_φ , H_ϑ , can be derived from the Potential $\mathbf{\Pi}_r$ via equation (1) and are related to the electric fields components E_φ and E_ϑ by the first Maxwell equation

$$\nabla \times \mathbf{H} = j\omega \epsilon_0 \mathbf{E}. \tag{37}$$

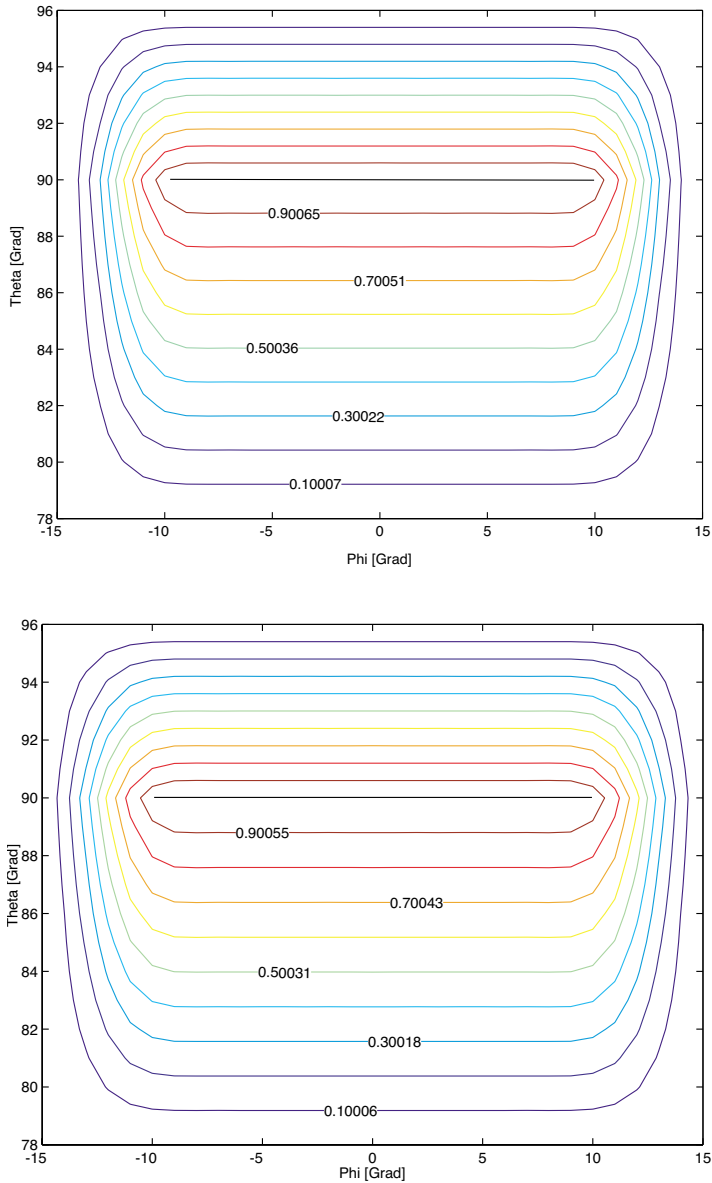


Figure 3. Isolines of the potential ($\Pi_r/[V]$) in the cross-section of a asymmetric GTEM cell. Obtained from the first solution (above) and from the second solution (below). The difference in the contour lines for both solutions at the plane $\vartheta = 90^\circ$ between septum and outer metal wall is due to numerical constrains and round off.

Fig. 3 shows the potential distribution as obtained from the calculation at any cross section of a 50 Ω -GTEM cell with the inner plate in an asymmetrical position. The geometrical data of the investigated cell are identical to those of the symmetric one (see table 1, sect. 3.2) with the difference in the height h_s of the septum; which, for the present case, is 44.63 cm. As can be seen from these figures, the equipotential lines portray the potential lines expected for these types of problems.

The solutions for the potential distribution presented above are exact and general. Furthermore they can be used for the calculation of the TEM mode in GTEM cells with any position of the septum as demonstrated. For practical applications however, the general Legendre functions and the derived new solution could be unwieldy even if the number m , because of the boundary conditions in the azimuthal direction at $\varphi = \pm\varphi_1$, is easy to calculate. It is therefore judicious, for the special case of symmetric cells, to look for a simple well-known solution. We deal with this aspect in the next subsection.

2.2. A Simple Approximation for the Special Case of Symmetric Cells

Since the GTEM cell has a small vertical angle ($\vartheta \leq 20^\circ$), it could be useful to take advantage of the symmetry in ϑ -direction for the case of symmetric cells.

Kleinwachter has shown in [16] that for conical horn with narrow vertical angle, the associated Legendre functions can be approximated by trigonometric functions. Piefke [17] confirmed this and showed that the maximal relative error for angle up to 30° is negligible. We therefore take inspiration from their works and derive the approximated solution for symmetric cells. Like Kleinwachter, let us set $\vartheta = \frac{\pi}{2}$, that is $\cot \vartheta = 0$ and $\sin \vartheta = 1$ in equation (6) and, with $\vartheta = \frac{\pi}{2} - \vartheta^*$, yields

$$\frac{\partial^2 D(\vartheta^*)}{\partial \vartheta^{*2}} - m^2 D(\vartheta^*) = 0. \quad (38)$$

Equation (38) is a classical differential equation which solutions are a combination of cosh- and sinh-functions

$$D(\vartheta^*) = A_1 \cosh(m\vartheta^*) + B_1 \sinh(m\vartheta^*). \quad (39)$$

From the boundary conditions on the surrounding metal walls at $\vartheta = \pm\vartheta_1^*$, an analogue relation as in equation (28) between the integration coefficients A_1 and B_1 can be derived. The general expression of the function $D(\vartheta)$ for the description of the potential in one region

is therefore

$$\begin{aligned}
 D_m(\vartheta^*) &= A_{1,m} \cdot \frac{\sin(m\vartheta_1^*) \cdot \cosh(m\vartheta^*) - \cosh(m\vartheta_1^*) \cdot \sinh(m\vartheta^*)}{\sinh(m\vartheta_1^*)} \\
 &= A_{1,m} \frac{\sinh[m(\vartheta_1^* - \vartheta^*)]}{\sinh(m\vartheta_1^*)}.
 \end{aligned}
 \tag{40}$$

From equation (3) the resulting potential is obtained

$$\Pi_r(\vartheta^*, \varphi) = \sum_{n=1}^{\infty} C_{m_n} \cdot \frac{\sinh[m_n(\vartheta_1^* - \vartheta^*)]}{\sinh(m_n\vartheta_1^*)} \cdot \cos(m_n\varphi), \tag{41}$$

where C_{m_n} denote new constants, which determination is dictated by the continuity boundary conditions between regions (1) and (2) and the value of the potential on the inner conductor. The numbers m_n are defined as in equation (28). The electric and magnetic field components can be obtained as in the previous section.

It is to remind that equation (41) is the common used solution for the TEM mode in TEM waveguides. Moreover, for/in the analysis in the section, the septum was placed at the equator in such way that ϑ fir the cell inner room varies between $90^\circ - \vartheta_1$ and $90^\circ + \vartheta_1$ (Fig. 4).

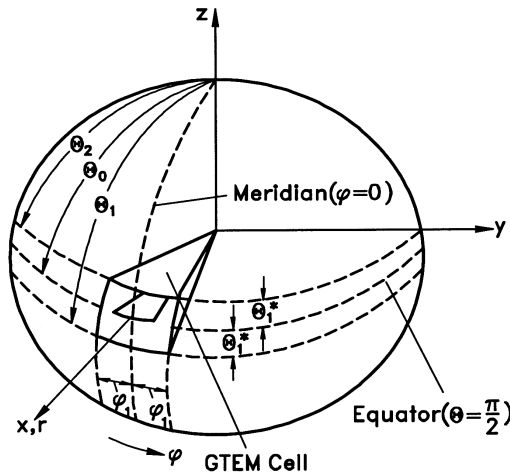


Figure 4. Position of the symmetric GTEM cell in the spherical coordinates. The cell was placed at the equator in such way that ϑ for the cell inner room varies between $90 - \vartheta_1^*$ and $90 + \vartheta_1^*$.

3. HIGHER-ORDER MODES IN UNLOADED CELLS

For the calculation of higher-order modes in the cell, quasi stationary conditions are no longer assumed. The potential $\mathbf{\Pi}_r$ should as such satisfied the Helmholtz equation in spherical co-ordinates.

$$\begin{aligned} \nabla^2 \mathbf{\Pi}_r - k^2 \mathbf{\Pi}_r &= 0 \\ \iff \frac{\partial^2 \mathbf{\Pi}_r}{\partial r^2} + \frac{1}{r^2 \sin \vartheta} \left[\frac{\partial}{\partial \vartheta} \left(\sin \vartheta \frac{\partial \mathbf{\Pi}_r}{\partial \vartheta} \right) + \frac{\partial}{\partial \varphi} \left(\frac{1}{\sin \vartheta} \frac{\partial \mathbf{\Pi}_r}{\partial \varphi} \right) \right] + k^2 \mathbf{\Pi}_r &= 0 \end{aligned} \quad (42)$$

To solve this partial differential equation, let us apply again the product solution method. The formulation

$$\mathbf{\Pi}_r = R(r) \cdot D(\vartheta) \cdot U(\varphi) \quad (43)$$

substituted in (42) leads to equation (44)

$$\begin{aligned} \frac{1}{R(r)} \frac{\partial^2 R(r)}{\partial r^2} + k^2 r^2 + \frac{1}{r^2 D(\vartheta) \sin \vartheta} \cdot \frac{\partial}{\partial \vartheta} \left(\sin \vartheta \cdot \frac{\partial D(\vartheta)}{\partial \vartheta} \right) \\ + \frac{1}{r^2 U(\varphi) \cdot \sin^2 \vartheta} \cdot \frac{\partial^2 U(\varphi)}{\partial \varphi^2} = 0, \end{aligned} \quad (44)$$

which may be, after multiplication by r^2 , separated in three ordinary independent differential equations (45) since R , D and U are functions of r , ϑ and φ respectively:

$$\begin{aligned} \frac{r^2}{R(r)} \cdot \frac{\partial^2 R(r)}{\partial r^2} + k^2 r^2 - n(n+1) &= 0, \quad (a) \\ \frac{\partial^2 U(\varphi)}{\partial \varphi^2} + m^2 U(\varphi) &= 0; \quad (b) \\ \frac{\partial^2 D(\vartheta)}{\partial \vartheta^2} + \cot \vartheta \cdot \frac{\partial D(\vartheta)}{\partial \vartheta} + \left[n(n+1) - \frac{m^2}{\sin^2 \vartheta} \right] D(\vartheta) &= 0; \quad (c) \end{aligned} \quad (45)$$

$n, m \in \mathbf{R}$

General Solutions of the equations (45) can be found in any standard book of fields and waves theory ([13] for example), and they are: For eq. (45a)

$$R(r) = \sqrt{kr} \mathcal{Z}_{n+\frac{1}{2}}(kr) \quad (46)$$

whereby $\mathcal{Z}_{n+\frac{1}{2}}(kr)$ are known forms of Bessel functions (Hankel functions for example).

For eq. (45b),

$$U(\varphi) = \left. \begin{matrix} \cos \\ \sin \end{matrix} \right\} (m\varphi) \quad (47)$$

and for eq. (45c), the well-known general solution is

$$D(\vartheta) = A \cdot P_n^m(\cos \vartheta) + B \cdot Q_n^m(\cos \vartheta) \quad (48)$$

whereby P_n^m and Q_n^m are the associated Legendre functions of the first and second kind respectively. For nonintegral values of n (we are expecting solutions for which $m + n \notin \mathbf{N}$) however, two independent solutions of (45c) are $P_n^m(\cos \vartheta)$ and $P_n^m(-\cos \vartheta)$. The function $D(\vartheta)$ therefore becomes

$$D(\vartheta) = A \cdot P_n^m(\cos \vartheta) + B \cdot P_n^m(-\cos \vartheta). \quad (49)$$

As a result, the expression for the potential $\mathbf{\Pi}_r$ is given by:

$$\begin{aligned} \mathbf{\Pi}_r(r, \vartheta, \varphi) &= \sqrt{kr} \mathcal{Z}_{n+\frac{1}{2}}(kr) \cdot [A \cdot P_n^m(\cos \vartheta) + B \cdot P_n^m(-\cos \vartheta)] \left. \begin{matrix} \cos \\ \sin \end{matrix} \right\} (m\varphi) \\ &= \sqrt{kr} \mathcal{Z}_{n+\frac{1}{2}}(kr) \cdot \mathcal{S}(\vartheta, \varphi), \end{aligned} \quad (50)$$

with

$$\mathcal{S}(\vartheta, \varphi) = [A \cdot P_n^m(\cos \vartheta) + B \cdot P_n^m(-\cos \vartheta)] \left. \begin{matrix} \cos \\ \sin \end{matrix} \right\} (m\varphi). \quad (51)$$

Equation (50) is general and valid for all geometrical structures which form can be described in spherical coordinates. The aim of this work however is to investigate field propagation in a GTEM cell, which is a conical coaxial wave-guide. It is therefore imperative to take into consideration the particularity of its geometry. For this purpose, we will, again, subdivide the cell in two regions (1) and (2) at the plane $\vartheta = \vartheta_0$, where the septum is placed (Fig. 2). (1) denotes the lower region and (2) indicates the upper one. ϑ_1 and ϑ_2 are as in the previous section, the lower and upper values of ϑ at the boundaries respectively. The potential $\mathbf{\Pi}_r$ can therefore be rewritten as

$$\begin{aligned} \mathbf{\Pi}_{(1,2)r}(r, \varphi, \vartheta) &= \sqrt{kr} \mathcal{Z}_{n+\frac{1}{2}}(kr) \\ &\cdot [A_{1,2} \cdot P_n^m(\cos \vartheta) + B_{1,2} \cdot P_n^m(-\cos \vartheta)] \left. \begin{matrix} \cos \\ \sin \end{matrix} \right\} (m\varphi) \\ &= \sqrt{kr} \mathcal{Z}_{n+\frac{1}{2}}(kr) \cdot \mathcal{S}_{1,2}(\vartheta, \varphi) \end{aligned} \quad (52)$$

for both regions.

3.1. Determination of the TM- and TE-Waves

Higher order modes can be derived from the following relations

$$\mathbf{E} = -j\mu_0\omega\nabla \times \mathbf{\Pi}_r \quad (\text{a}) \quad \mathbf{H} = k^2\mathbf{\Pi}_r + \nabla(\nabla\mathbf{\Pi}_r) \quad (\text{b}) \quad (53)$$

that is

$$\begin{aligned} E_r &= 0, & H_r &= k^2\mathbf{\Pi}_r + \frac{\partial^2\mathbf{\Pi}_r}{\partial r^2} \\ E_\vartheta &= -j\frac{\mu_0\omega}{r\sin\vartheta}\frac{\partial\mathbf{\Pi}_r}{\partial\varphi}; & H_\vartheta &= \frac{1}{r}\frac{\partial^2\mathbf{\Pi}_r}{\partial r\partial\vartheta} \\ E_\varphi &= j\frac{\mu_0\omega}{r}\frac{\partial\mathbf{\Pi}_r}{\partial\vartheta}; & H_\varphi &= \frac{1}{r\sin\vartheta}\frac{\partial^2\mathbf{\Pi}_r}{\partial r\partial\varphi} \end{aligned} \quad (54)$$

for the TE-waves and

$$\mathbf{H} = -j\omega\varepsilon_0\nabla \times \mathbf{\Pi}_r \quad (\text{a}) \quad \mathbf{E} = k^2\mathbf{\Pi}_r + \nabla(\nabla\mathbf{\Pi}_r) \quad (\text{b}) \quad (55)$$

that is

$$\begin{aligned} H_r &= 0, & E_r &= k^2\mathbf{\Pi}_r + \frac{\partial^2\mathbf{\Pi}_r}{\partial r^2} \\ H_\vartheta &= j\frac{\omega\varepsilon_0}{r\sin\vartheta}\frac{\partial\mathbf{\Pi}_r}{\partial\varphi}; & E_\vartheta &= \frac{1}{r}\frac{\partial^2\mathbf{\Pi}_r}{\partial r\partial\vartheta} \\ H_\varphi &= -j\frac{\omega\varepsilon_0}{r}\frac{\partial\mathbf{\Pi}_r}{\partial\vartheta}; & E_\varphi &= \frac{1}{r\sin\vartheta}\frac{\partial^2\mathbf{\Pi}_r}{\partial r\partial\varphi} \end{aligned} \quad (56)$$

for TM modes.

Since the determination of explicit expressions of the above fields is closely related to the potential, it is convenient to express the potential in a more closed-form. Closed-form expressions for the potential solution (52) are obtained through the boundary conditions. These require that the tangential components of the electrical field and the normal components of the magnetic field shall vanish on surrounding metal walls (contour C).

For the TE modes, this means that the potential shall satisfy the Neumann's boundary condition

$$\frac{\partial\mathbf{\Pi}_{(1,2)r}^{TE}}{\partial n} = 0 \iff \frac{\partial\mathcal{S}_{1,2}^{TE}(\varphi, \vartheta)}{\partial n} = 0 \quad \text{on } C \quad (57)$$

whereas for the TM waves, the potential shall fulfill the Dirichlet's boundary condition

$$\mathbf{\Pi}_{(1,2)r}^{TM} = 0 \iff \mathcal{S}_{1,2}^{TM}(\varphi, \vartheta) = 0 \quad \text{on } C. \quad (58)$$

From the boundary conditions in the azimuthal direction, the number m can be determined. In fact we have $U(\pm\varphi_1) = 0$, i.e.,

$$\left. \begin{matrix} \cos \\ \sin \end{matrix} \right\} (m\varphi_1) = 0 \Rightarrow m_\nu = \frac{\nu \cdot \pi}{2\varphi_1}, \quad (59)$$

with $\nu = 0, 1, 2, 3, \dots$ for TE waves and $\nu = 1, 2, 3, \dots$ for TM modes.

Solving eqs. (57) and (58) along the planes $\vartheta = \vartheta_1$ and $\vartheta = \vartheta_2$ with respect to $B_{(1,2)}$ ($A_{(1,2)}$ are assumed to be parameters), lead to

$$\begin{aligned} S_{(1,2)n}^{TE,m_\nu}(\vartheta, \varphi) = & A_{(1,2)n}^{TE,m_\nu} \frac{P_n^{m_\nu}(-\cos\vartheta_{1,2}) \cdot P_n^{m_\nu}(\cos\vartheta) - P_n^{m_\nu}(\cos\vartheta_{1,2}) \cdot P_n^{m_\nu}(-\cos\vartheta)}{P_n^{m_\nu}(-\cos\vartheta_{1,2})} \\ & \cdot \left. \begin{matrix} \cos \\ \sin \end{matrix} \right\} (m_\nu\varphi) \end{aligned} \quad (60)$$

for TE-waves and

$$\begin{aligned} S_{(1,2)n}^{TM,m_\nu}(\vartheta, \varphi) = & A_{(1,2)n}^{TM,m_\nu} \frac{P_n^{m_\nu}(-\cos\vartheta_{1,2}) \cdot P_n^{m_\nu}(\cos\vartheta) - P_n^{m_\nu}(\cos\vartheta_{1,2}) \cdot P_n^{m_\nu}(-\cos\vartheta)}{P_n^{m_\nu}(-\cos\vartheta_{1,2})} \\ & \cdot \left. \begin{matrix} \cos \\ \sin \end{matrix} \right\} (m_\nu\varphi) \end{aligned} \quad (61)$$

for TM-waves. General expressions for the potential Π_r are obtained by setting eqs. (60) and (61) in (50). We therefore have

$$\begin{aligned} \Pi_{(1,2)r}^{TE}(r, \vartheta, \varphi) = & A_{(1,2)n}^{TE,m_\nu} \cdot \frac{\sqrt{kr} Z_{n+1/2}(kr)}{P_n^{m_\nu}(-\cos\vartheta_{1,2})} [P_n^{m_\nu}(-\cos\vartheta_{1,2})P_n^{m_\nu}(\cos\vartheta) \\ & - P_n^{m_\nu}(\cos\vartheta_{1,2}) \cdot P_n^{m_\nu}(-\cos\vartheta)] \cdot \left. \begin{matrix} \cos \\ \sin \end{matrix} \right\} (m_\nu\varphi) \end{aligned} \quad (62)$$

for TE waves and

$$\begin{aligned} \Pi_{(1,2)r}^{TM}(r, \vartheta, \varphi) = & A_{(1,2)n}^{TM,m_\nu} \cdot \frac{\sqrt{kr} Z_{n+1/2}(kr)}{P_n^{m_\nu}(-\cos\vartheta_{1,2})} [P_n^{m_\nu}(-\cos\vartheta_{1,2}) \cdot P_n^{m_\nu}(\cos\vartheta) \\ & - P_n^{m_\nu}(\cos\vartheta_{1,2}) \cdot P_n^{m_\nu}(-\cos\vartheta)] \cdot \left. \begin{matrix} \cos \\ \sin \end{matrix} \right\} (m_\nu\varphi). \end{aligned} \quad (63)$$

for TM waves. In the above formulas, the subscripts (1) and (2) denote the lower and upper region of the cell respectively, n is the index of the Legendre function, m_ν , is defined as above.

Explicit expressions of the field components are given in the appendix. $A_{(1,2)n}^{TE,m_\nu}$ and $A_{(1,2)n}^{TM,m_\nu}$ have to be defined. Their determination is dictated by the continuity limit conditions between regions (1) and (2) at the plane $\vartheta = \vartheta_0$ in the gape regions between the end of the septum and the metal walls and, the value of the potential on the inner conductor as well

On the inner conductor, the same conditions for the electrical and magnetic field as on the outer metal walls are required. This means that

$$\frac{\partial \mathbf{\Pi}_{(1,2)r}^{(TE)}}{\partial n} = 0 \iff \frac{\partial \mathcal{S}_{1,2}^{TE}(\varphi, \vartheta)}{\partial \vartheta} = 0, \quad (\text{a}) \quad (64)$$

$$\mathbf{\Pi}_{(1,2)r}^{(TM)} = 0 \iff \mathcal{S}_{1,2}^{TM}(\varphi, \vartheta) = 0, \quad (\text{b})$$

both for $-\varphi_s \leq \varphi \leq \varphi_s$.

The continuity of the fields in the gap regions means that the potential and its derivative normal to the plane $\vartheta = \vartheta_0$ should be continuous for TM waves on the one side and on the other side the potential as well as its derivatives parallel and normal to the plane $\vartheta = \vartheta_0$ have to be continuous. Since, by imposing the continuity of the potential in the gap regions, the continuity of its parallel derivative to the plane $\vartheta = \vartheta_0$ is automatically satisfied, this last condition is redundant. Therefore the conditions to impose on the potential and its derivatives for the TM case are reduced to the same as for the TE waves. As a result, four additional equations in each case are obtained

$$\mathbf{\Pi}_{1r}^{(TE,TM)} = \mathbf{\Pi}_{2r}^{(TE,TM)} \iff \mathcal{S}_1^{(TE,TM)}(\varphi, \vartheta) = \mathcal{S}_2^{(TE,TM)}(\varphi, \vartheta) \quad \text{for } -\varphi_1 \leq \varphi \leq -\varphi_s \quad \text{and} \quad \varphi_s \leq \varphi \leq \varphi_1 \quad (65)$$

$$\frac{\partial \mathbf{\Pi}_{1r}^{(TE,TM)}}{\partial \vartheta} = \frac{\partial \mathbf{\Pi}_{2r}^{(TE,TM)}}{\partial \vartheta} \iff \frac{\partial \mathcal{S}_1^{(TE,TM)}(\varphi, \vartheta)}{\partial \vartheta} = \frac{\partial \mathcal{S}_2^{(TE,TM)}(\varphi, \vartheta)}{\partial \vartheta} \quad \text{for } -\varphi_1 \leq \varphi \leq -\varphi_s \quad \text{and} \quad \varphi_s \leq \varphi \leq \varphi_1. \quad (66)$$

By means of the symmetry in the φ direction, these equations are reduced to two equations. With equations (64) we have a set of four equations for the TE and TM case as well.

At this stage, the incoming development will be only hold for TM waves since an analogous analysis can be carried out for TE waves. Results for TE waves are given later without any particular derivation.

For TM waves, this set of four equations is

$$A_{1n}^{TM,m_\nu} \cdot \mathcal{N}_n^{m_\nu}(\cos \vartheta_0) \cdot \left. \begin{array}{l} \cos \\ \sin \end{array} \right\} (m_\nu \varphi) = 0 \quad (\text{a})$$

$$A_{2n}^{TM,m_\nu} \cdot \mathcal{W}_n^{m_\nu}(\cos \vartheta_0) \cdot \frac{\cos}{\sin} \left\} (m_\nu \varphi) = 0 \tag{b}$$

$$\text{both for } 0 \leq \varphi \leq \varphi_s \tag{67}$$

$$\left[A_{1n}^{TM,m_\nu} \cdot \mathcal{N}_n^{m_\nu}(\cos \vartheta_0) - A_{2n}^{TM,m_\nu} \cdot \mathcal{W}_n^{m_\nu}(\cos \vartheta_0) \right] \cdot \frac{\cos}{\sin} \left\} (m_\nu \varphi) = 0 \tag{c}$$

$$\left[A_{1n}^{TM,m_\nu} \cdot \mathcal{N}'_n{}^{m_\nu}(\cos \vartheta_0) - A_{2n}^{TM,m_\nu} \cdot \mathcal{W}'_n{}^{m_\nu}(\cos \vartheta_0) \right] \cdot \frac{\cos}{\sin} \left\} (m_\nu \varphi) = 0 \tag{d}$$

the two last equations are valid for $\varphi_s \leq \varphi \leq \varphi_1$.

In equations (67) $\mathcal{N}_n^{m_\nu}$ and $\mathcal{W}_n^{m_\nu}$ in are defined as follow

$$\mathcal{N}_n^{m_\nu}(\cos \vartheta) = \frac{P_n^{m_\nu}(-\cos \vartheta_1) \cdot P_n^{m_\nu}(\vartheta) - P_n^{m_\nu}(\cos \vartheta_1) \cdot P_n^{m_\nu}(-\cos \vartheta)}{P_n^{m_\nu}(\cos \vartheta_1)} \tag{68}$$

$$\mathcal{W}_n^{m_\nu}(\cos \vartheta) = \frac{P_n^{m_\nu}(-\cos \vartheta_2) \cdot P_n^{m_\nu}(\vartheta) - P_n^{m_\nu}(\cos \vartheta_2) \cdot P_n^{m_\nu}(-\cos \vartheta)}{P_n^{m_\nu}(\cos \vartheta_2)} \tag{69}$$

$\mathcal{N}'_n{}^{m_\nu}$ and $\mathcal{W}'_n{}^{m_\nu}$ are their derivative with respect to ϑ . Deriving A_{2n}^{TM,m_ν} from eq. (67c) and setting it in (67b) leads to eq. (70)

$$A_{1n}^{TM,m_\nu} \cdot \mathcal{N}'_n{}^{m_\nu}(\cos \vartheta) \cdot \frac{\cos}{\sin} \left\} (m_\nu \varphi) = 0 \tag{70}$$

which is equivalent to equation (67a) and, therefore redundant. Furthermore, by replacing A_{2n}^{TM,m_ν} in eq. (67d) by its expression obtained from equation (67c), we have

$$A_{1n}^{TM,m_\nu} \frac{\mathcal{N}_n^{m_\nu}(\cos \vartheta_0) \cdot \mathcal{W}_n^{m_\nu}(\cos \vartheta_0) - \mathcal{W}_n^{m_\nu}(\cos \vartheta_0) \cdot \mathcal{N}_n^{m_\nu}(\cos \vartheta_0)}{\mathcal{W}_n^{m_\nu}(\cos \vartheta_0)} \cdot \frac{\cos}{\sin} \left\} (m_\nu \varphi) = 0, \quad \text{for } \varphi_s < \varphi < \varphi_1. \tag{71}$$

After suppression of the redundant equation (67b), the set of equations (67) is reduced to the following system of equations

$$A_{1n}^{TM,m_\nu} \cdot \mathcal{N}_n^{m_\nu}(\cos \vartheta_0) \cdot \frac{\cos}{\sin} \left\} (m_\nu \varphi) = 0 \quad \text{for } 0 \leq \varphi \leq \varphi_s \tag{a}$$

$$\tag{72}$$

$$A_{1n}^{TM,m\nu} \frac{\mathcal{N}_n^{m\nu}(\cos \vartheta_0) \cdot \mathcal{W}_n^{m\nu}(\cos \vartheta_0) - \mathcal{W}_n^{m\nu}(\cos \vartheta_0) \cdot \mathcal{N}_n^{m\nu}(\cos \vartheta_0)}{\mathcal{W}_n^{m\nu}(\cos \vartheta_0)} \cdot \left. \begin{matrix} \cos \\ \sin \end{matrix} \right\} (m\nu\varphi) = 0, \quad \text{for } \varphi_s < \varphi < \varphi_1 \quad (\text{b})$$

Let us now consider the two well know art of cells: the symmetric cell and the asymmetric one separately.

The symmetric cell as depicted in Fig. 4. In this case, the second equation (72b) is superfluous and is therefore to eliminate, since $\mathcal{N}_n^{m\nu}(\cos \vartheta) = \mathcal{W}_n^{m\nu}(\cos \vartheta)$. The determination of the index n is reduced to search of the solution of the transcendental equation

$$L_n^{m\nu}(\cos \vartheta_0) = P_n^{m\nu}(-\cos \vartheta_1) \cdot P_n^{m\nu}(\cos \vartheta_0) - P_n^{m\nu}(\cos \vartheta_1) \cdot P_n^{m\nu}(-\cos \vartheta_0) = 0. \quad (73)$$

Equation (73) can be solved numerically.

The asymmetric cell For this case, it is convenient to make used of the point-matching method [18] by considering a number of M points on the inner conductor where equation (72a) has to be fulfilled and a number of $(N - M)$ points between the septum and the outer metal at the boundary between region (1) and region (2) where equation should to be fulfilled. That is

$$\sum_n A_{1n}^{TM,m\nu} \mathcal{N}_n^{m\nu}(\cos \vartheta_0) \cdot \left. \begin{matrix} \cos \\ \sin \end{matrix} \right\} (m\nu\varphi_i) = 0 \quad \text{for } 0 \leq \varphi_i \leq \varphi_s, \quad i = 1, \dots, M \quad (\text{a}) \quad (74)$$

$$\sum_n A_{1n}^{TM,m\nu} \frac{\mathcal{N}_n^{m\nu}(\cos \vartheta_0) \cdot \mathcal{W}_n^{m\nu}(\cos \vartheta_0) - \mathcal{W}_n^{m\nu}(\cos \vartheta_0) \cdot \mathcal{N}_n^{m\nu}(\cos \vartheta_0)}{\mathcal{W}_n^{m\nu}(\cos \vartheta_0)} \cdot \left. \begin{matrix} \cos \\ \sin \end{matrix} \right\} (m\nu\varphi_i) = 0, \quad \text{for } \varphi_s < \varphi_i < \varphi_1, \quad i = M + 1, \dots, N \quad (\text{b})$$

The index n is given by values of n for which the determinant of the system of equations (74) is equal to zero.

A similar development as for equations (67) to (74) can be hold for TE waves. As for the TM waves, it can be shown that the determination of the index n is reduced to the solution of the transcendental equation

$$L_n^{m\nu}(\cos \vartheta_0) = P_n^{m\nu}(-\cos \vartheta_1) \cdot P_n^{m\nu}(\cos \vartheta_0) - P_n^{m\nu}(\cos \vartheta_1) \cdot P_n^{m\nu}(-\cos \vartheta_0) = 0, \quad (75)$$

in case of symmetric cells and, for asymmetric cells, n are values of n for which the determinant of the system of equations (76) is zero.

$$\sum_n A_{1n}^{TE,m\nu} \mathcal{N}_n^{m\nu}(\cos \vartheta_0) \cdot \left. \begin{matrix} \cos \\ \sin \end{matrix} \right\} (m\nu\varphi_i) = 0$$

$$\text{for } 0 \leq \varphi_i \leq \varphi_s, \quad i = 1, \dots, M \quad (\text{a})$$

$$(76)$$

$$\sum_n A_{1n}^{TE,m\nu} \frac{\mathcal{N}_n^{m\nu}(\cos \vartheta_0) \cdot \mathcal{W}_n^{\prime m\nu}(\cos \vartheta_0) - \mathcal{N}_n^{\prime m\nu}(\cos \vartheta_0) \cdot \mathcal{W}_n^{m\nu}(\cos \vartheta_0)}{\mathcal{W}_n^{\prime m\nu}(\cos \vartheta_0)}$$

$$\cdot \left. \begin{matrix} \cos \\ \sin \end{matrix} \right\} (m\nu\varphi_i) = 0, \quad \text{for } \varphi_s < \varphi_i < \varphi_1, \quad i = M + 1, \dots, N \quad (\text{b})$$

where $\mathcal{N}_n^{m\nu}$ and $\mathcal{W}_n^{m\nu}$ are

$$\mathcal{N}_n^{m\nu}(\cos \vartheta) = \frac{P_n^{m\nu}(-\vartheta_1) \cdot P_n^{m\nu}(\vartheta) - P_n^{m\nu}(\vartheta_1) \cdot P_n^{m\nu}(-\vartheta)}{P_n^{\prime m\nu}(\vartheta_1)} \quad (77)$$

$$\mathcal{W}_n^{m\nu}(\cos \vartheta) = \frac{P_n^{m\nu}(-\vartheta_2) \cdot P_n^{m\nu}(\vartheta) - P_n^{\prime m\nu}(\vartheta_2) \cdot P_n^{m\nu}(-\vartheta)}{P_n^{\prime m\nu}(\vartheta_2)} \quad (78)$$

$\mathcal{N}_n^{\prime m\nu}$ and $\mathcal{W}_n^{\prime m\nu}$ are, as defined above, their derivative with respect to ϑ .

3.2. Cutoff Phenomena and Resonance Frequencies

Let us imagine one of the lowest-order mode[†] propagating radially inward in the cell. Although modified by the convergence of the sides, this mode will be only slightly different to the TE₁₀ mode of the rectangular wave guide. We would consequently expect a cutoff phenomenon at such a point where the radial field impedance becomes predominantly reactive [12]. The radial field impedance for an inward traveling wave is in general given by

$$\underline{Z}_{-}^{(TE)} = \left(\frac{E_{\vartheta}}{H_{\varphi}} \right)_{-} = -j\mu_0\omega \frac{k\sqrt{kr} \cdot Z_{\eta}(kr)}{\frac{d}{dr}(\sqrt{kr}Z_{\eta}(kr))} = R_{\eta} - jX_{\eta}, \quad (79)$$

where $\eta = n + 1/2$ and Z_{η} is the Hankel functions of first kind. This impedance becomes predominantly reactive at a value $kr = \sqrt{\eta(\eta + 1)}$.

[†] It is assumed here that the lowest higher-order mode propagating in the cell is the TE₁₀ mode although this is not always the case, since the TE₀₁ mode can, depending on the degree of the asymmetry, also propagates as first higher-order mode within the cell [3]. This point does not however affects the validity and generality of the demonstration.

From the relations $kr = \sqrt{\eta(\eta + 1)}$ and $k = 2\pi\sqrt{\varepsilon_0\mu_0}f$, the cutoff frequency can be obtained. It is given by

$$f_c = \frac{\sqrt{\eta(\eta + 1)}}{2\pi r\sqrt{\varepsilon_0\mu_0}}, \quad (80)$$

where r is the distance from the apex. Equation (80) can be reduced to $f_c = \frac{\eta}{2\pi r\sqrt{\varepsilon_0\mu_0}}$ for large values of n or η .

Table 1. Calculated cutoff frequencies (left) and resonance frequencies (right) of some higher-order modes in a symmetric cell at a distance $r = 210$ cm from the apex. Cell's geometrical data at this distance: total height of the cell in the test zone: $b = 68.23$ cm, width of the cell: $a = 112.538$ cm, width of the septum: $b_s = 65$ cm, height of the septum: $h_s = 34.11$ cm.

Type	f_c [MHz]	Type	f_r [MHz]
TE ₁₀	158.65	TE ₁₀₁	230.91
TE ₁₁	204.29	TE ₁₀₂	312.09
TE ₂₀	204.26	TE ₁₁₁	281.05
TE ₂₁	249.80	TE ₁₁₂	365.66
TE ₁₂	250.00	TM ₁₁₁	289.73
TM ₁₁	212.267		

Resonance frequencies are their side obtained at radii where the radial field impedance becomes predominantly active. These radii are points where the imaginary part X_η is zero. In our case, since the origin is included, resonance frequencies are roots of Bessel functions of first kind, for an inward propagating wave. In fact, the equation to be solved is

$$-16j\varepsilon_0\mu_0^2\pi^3\frac{b}{\vartheta}f^3 \cdot J_{n+\frac{1}{2}}\left(2\pi b\frac{\sqrt{\varepsilon_0\mu_0}}{\vartheta}f\right) = 0, \quad (81)$$

where r has been substitute by b/ϑ . ϑ and b are the vertical angle and the total height of the cell in the test zone respectively.

In case of TM waves, the radial impedance is given by

$$\underline{Z}_-^{(TM)} = -\frac{\frac{d}{dr}\left(\sqrt{kr} \cdot \mathcal{Z}_\eta(kr)\right)}{j\varepsilon_0\omega k\sqrt{kr}\mathcal{Z}_\eta(kr)}. \quad (82)$$

Consequently, resonance frequencies are given by the roots of equation

(83).

$$j \left[(2\pi\sqrt{\varepsilon_0\mu_0}f + 2n + 1) \cdot J_{n+\frac{1}{2}} \left(2\pi\frac{b}{\vartheta}\sqrt{\mu_0\varepsilon_0}f \right) - 4\frac{b}{\vartheta}\pi\sqrt{\varepsilon_0\mu_0}f \cdot J_{n+\frac{3}{2}} \left(2\frac{b}{\vartheta}\pi\sqrt{\varepsilon_0\mu_0}f \right) \right] = 0 \quad (83)$$

Calculated cut-off and first resonance frequencies are reported in Table 1.

4. CONCLUSION

This work analyzes the propagation of the spherical TEM and higher order modes in GTEM cells. Two general closed-form solutions for the principal waves are derived. These expressions are fairly simple and can be implemented on personal computers. Moreover, as have been shown, they can be agreeably combined with the common spherical and cylindrical functions in determining higher order modes in loaded and unloaded cells. For symmetric cells, substantial simplification in the analysis has been obtained for the determination of local higher order modes. For asymmetric cells, the matching-points method has been applied. The method presented leads to an easier and accurate calculation of cutoff and resonance frequencies.

ACKNOWLEDGMENT

The author would like to thank the reviewers who generously shared their knowledge and viewpoints. Their comments were helpful.

APPENDIX A. CALCULATION OF THE FIELD'S COMPONENTS FROM THE POTENTIAL Π_r

As stated in Section 2.2, the magnetic field's components H_φ and H_ϑ can be derived from the equations. From equation (1) we have

$$H_\varphi = -\frac{1}{r} \frac{\partial \Pi_r}{\partial \vartheta} \quad \text{and} \quad H_\vartheta = \frac{1}{r \cdot \sin \vartheta} \frac{\partial \Pi_r}{\partial \varphi}. \quad (A1)$$

which results in the following explicit expressions

$$H_{(1,2)\varphi} = -\frac{1}{r} \sum_{n=1}^{\infty} C_{1,2}^{m_n} \frac{\mathcal{Q}_0^{m_n}(\cos \vartheta_{1,2}) \mathcal{P}_0^{m_n}(\cos \vartheta) - \mathcal{P}_0^{m_n}(\cos \vartheta_{1,2}) \mathcal{Q}_0^{m_n}(\cos \vartheta)}{\mathcal{Q}_0^{m_n}(\cos \vartheta_{1,2})}$$

$$\cdot \cos(m_n \varphi) \cdot e^{-j\beta_0 r} \quad (\text{a})$$

$$(A2)$$

$$H_{(1,2)\vartheta} =$$

$$-\frac{1}{r \sin \vartheta} \sum_{n=1}^{\infty} m_n C_{1,2}^{m_n} \frac{\mathcal{Q}_0^{m_n}(\cos \vartheta_{1,2}) \mathcal{P}_0^{m_n}(\cos \vartheta) - \mathcal{P}_0^{m_n}(\cos \vartheta_{1,2}) \mathcal{Q}_0^{m_n}(\cos \vartheta)}{\mathcal{Q}_0^{m_n}(\cos \vartheta_{1,2})}$$

$$\cdot \sin(m_n \varphi) \cdot e^{-j\beta_0 r} \quad (\text{b})$$

The primes in (A2a) denote the derivative. From the relation (37) between the magnetic and the electric field, we have $E_{(1,2)\varphi} = -Z_0 \cdot H_{(1,2)\vartheta}$ and $E_{(1,2)\vartheta} = Z_0 \cdot H_{(1,2)\varphi}$ i.e.,

$$E_{(1,2)\varphi} =$$

$$\frac{Z_0}{r \sin \vartheta} \sum_{n=1}^{\infty} m_n C_{1,2}^{m_n} \frac{\mathcal{Q}_0^{m_n}(\cos \vartheta_{1,2}) \mathcal{P}_0^{m_n}(\cos \vartheta) - \mathcal{P}_0^{m_n}(\cos \vartheta_{1,2}) \mathcal{Q}_0^{m_n}(\cos \vartheta)}{\mathcal{Q}_0^{m_n}(\cos \vartheta_{1,2})}$$

$$\cdot \sin(m_n \varphi) \cdot e^{-j\beta_0 r} \quad (\text{a})$$

$$(A3)$$

$$E_{(1,2)\vartheta} =$$

$$-\frac{Z_0}{r} \sum_{n=1}^{\infty} C_{1,2}^{m_n} \frac{\mathcal{Q}_0^{m_n}(\cos \vartheta_{1,2}) \mathcal{P}_0^{m_n}(\cos \vartheta) - \mathcal{P}_0^{m_n}(\cos \vartheta_{1,2}) \mathcal{Q}_0^{m_n}(\cos \vartheta)}{\mathcal{Q}_0^{m_n}(\cos \vartheta_{1,2})}$$

$$\cdot \cos(m_n \varphi) \cdot e^{-j\beta_0 r} \quad (\text{b})$$

In (A2) to (A3) $\beta_0 = \omega \sqrt{\varepsilon_0 \mu_0}$ and $Z_0 = 377 \Omega$. The above relations are from the first solution given in Section 2.1.1. From the alternative solution we have the equations (A4a)–(A5b) stated below for H_φ , H_ϑ , E_ϑ and E_φ respectively.

$$H_{(1,2)\varphi} = -\frac{1}{r} \sum_{n=1}^{\infty} \left\{ A_{1,2}^{m_n} \frac{1}{2} m_n^2 \left[\ln \frac{\left| \tan \frac{\vartheta}{2} \right|}{\frac{\vartheta}{2}} - 1 + \frac{2\vartheta}{\sin \frac{\vartheta}{4}} \right. \right.$$

$$\left. - \sum_{k=1}^{\infty} \frac{2^{2k} (2^{2k-1} - 1) B_k}{k(2k)!} \left(\frac{\vartheta}{2} \right)^{2k} \right] + C_{1,2}^{m_n} \frac{2}{\sin \frac{\vartheta}{4}} \left. \right\}$$

$$\cdot \cos(m_n \varphi) \cdot e^{-j\beta_0 r}, \quad (\text{a})$$

$$(A4)$$

$$\begin{aligned}
 H_{(1,2)\vartheta} = & -\frac{1}{r \sin \vartheta} \sum_{n=1}^{\infty} \left\{ A_{m_n}^{(1,2)} \left\{ \frac{1}{2} m_n^2 \left[\vartheta \left(\ln \frac{\left| \tan \frac{\vartheta}{2} \right|}{\frac{\vartheta}{2}} + 1 \right) \right. \right. \right. \\
 & - \vartheta_{1,2} \left(\ln \frac{\left| \tan \frac{\vartheta_{1,2}}{2} \right|}{\frac{\vartheta_{1,2}}{2}} + 1 \right) + \sum_{k=1}^{\infty} \frac{2^{2k+1} (2^{2k-1} - 1) B_k}{k(2k+1)!} \\
 & \cdot \left[\left(\frac{\vartheta_{1,2}}{2} \right)^{2k+1} - \left(\frac{\vartheta}{2} \right)^{2k+1} \right] \left. \right\} + C_{m_n}^{(1,2)} \ln \frac{\left| \tan \frac{\vartheta}{2} \right|}{\left| \tan \frac{\vartheta_{1,2}}{2} \right|} \left. \right\} \\
 & \cdot \cos(m_n \phi) \cdot e^{-j\beta_0 r}, \tag{b}
 \end{aligned}$$

$$\begin{aligned}
 E_{(1,2)\vartheta} = & -\frac{Z_0}{r} \sum_{n=1}^{\infty} \left\{ A_{1,2}^{m_n} \frac{1}{2} m_n^2 \left[\ln \frac{\left| \tan \frac{\vartheta}{2} \right|}{\frac{\vartheta}{2}} - 1 + \frac{2\vartheta}{\sin \frac{\vartheta}{4}} \right. \right. \\
 & - \left. \left. \sum_{k=1}^{\infty} \frac{2^{2k} (2^{2k-1} - 1) B_k}{k(2k)!} \left(\frac{\vartheta}{2} \right)^{2k} \right] + C_{1,2}^{m_n} \frac{2}{\sin \frac{\vartheta}{4}} \right\} \\
 & \cdot \cos(m_n \varphi) \cdot e^{-j\beta_0 r}, \tag{a}
 \end{aligned}$$

(A5)

$$\begin{aligned}
 E_{(1,2)\vartheta} = & \frac{Z_0}{r \sin \vartheta} \sum_{n=1}^{\infty} \left\{ A_{m_n}^{(1,2)} \left\{ \frac{1}{2} m_n^2 \left[\vartheta \left(\ln \frac{\left| \tan \frac{\vartheta}{2} \right|}{\frac{\vartheta}{2}} + 1 \right) \right. \right. \right. \\
 & - \vartheta_{1,2} \left(\ln \frac{\left| \tan \frac{\vartheta_{1,2}}{2} \right|}{\frac{\vartheta_{1,2}}{2}} + 1 \right) + \sum_{k=1}^{\infty} \frac{2^{2k+1} (2^{2k-1} - 1) B_k}{k(2k+1)!} \\
 & \cdot \left[\left(\frac{\vartheta_{1,2}}{2} \right)^{2k+1} - \left(\frac{\vartheta}{2} \right)^{2k+1} \right] \left. \right\} + C_{m_n}^{(1,2)} \ln \frac{\left| \tan \frac{\vartheta}{2} \right|}{\left| \tan \frac{\vartheta_{1,2}}{2} \right|} \left. \right\} \\
 & \cdot \cos(m_n \phi) \cdot e^{-j\beta_0 r}, \tag{b}
 \end{aligned}$$

Field components for higher order modes are

$$E_{(1,2)r} = 0$$

$$E_{(1,2)\vartheta} = -A_{(1,2)n}^{TE,m_\nu} \cdot j \frac{\mu_0 \omega}{r \sin \vartheta} \cdot \frac{\sqrt{kr} \mathcal{Z}_{n+1/2}(kr)}{P_n^{m_\nu}(-\cos \vartheta_{1,2})} [P_n^{m_\nu}(-\cos \vartheta_{1,2}) \cdot P_n^{m_\nu}(\cos \vartheta) - P_n^{m_\nu}(\cos \vartheta_{1,2}) \cdot P_n^{m_\nu}(-\cos \vartheta)] \left(\frac{\cos}{\sin} \right) (m_\nu \varphi)'$$

$$E_{(1,2)\varphi} = A_{(1,2)n}^{TE,m_\nu} \cdot j \frac{\mu_0 \omega}{r} \cdot \frac{\sqrt{kr} \mathcal{Z}_{n+1/2}(kr)}{P_n^{m_\nu}(-\cos \vartheta_{1,2})} [P_n^{m_\nu}(-\cos \vartheta_{1,2}) \cdot P_n^{m_\nu}(\cos \vartheta) - P_n^{m_\nu}(\cos \vartheta_{1,2}) \cdot P_n^{m_\nu}(-\cos \vartheta)] \frac{\cos}{\sin} (m_\nu \varphi)$$

$$H_{(1,2)r} = A_{(1,2)n}^{TE,m_\nu} \cdot \frac{kn(n+1)}{(kr)^2} \cdot \frac{\sqrt{kr} \mathcal{Z}_{n+1/2}(kr)}{P_n^{m_\nu}(-\cos \vartheta_{1,2})} [P_n^{m_\nu}(-\cos \vartheta_{1,2}) \cdot P_n^{m_\nu}(\cos \vartheta) - P_n^{m_\nu}(\cos \vartheta_{1,2}) \cdot P_n^{m_\nu}(-\cos \vartheta)] \frac{\cos}{\sin} (m_\nu \varphi)$$

$$H_{(1,2)\vartheta} = A_{(1,2)n}^{TE,m_\nu} \cdot \frac{1}{kr} \cdot \frac{(\sqrt{kr} \mathcal{Z}_{n+1/2}(kr))'}{P_n^{m_\nu}(-\cos \vartheta_{1,2})} [P_n^{m_\nu}(-\cos \vartheta_{1,2}) \cdot P_n^{m_\nu}(\cos \vartheta) - P_n^{m_\nu}(\cos \vartheta_{1,2}) \cdot P_n^{m_\nu}(-\cos \vartheta)] \frac{\cos}{\sin} (m_\nu \varphi) \quad (A6)$$

$$H_{(1,2)\varphi} = -A_{(1,2)n}^{TE,m_\nu} \cdot \frac{1}{kr \sin \vartheta} \cdot \frac{(\sqrt{kr} \mathcal{Z}_{n+1/2}(kr))'}{P_n^{m_\nu}(-\cos \vartheta_{1,2})} [P_n^{m_\nu}(-\cos \vartheta_{1,2}) \cdot P_n^{m_\nu}(\cos \vartheta) - P_n^{m_\nu}(\cos \vartheta_{1,2}) \cdot P_n^{m_\nu}(-\cos \vartheta)] \left(\frac{\cos}{\sin} \right) (m_\nu \varphi)'$$

for TE-waves, and

$$H_{(1,2)r} = 0$$

$$H_{(1,2)\vartheta} = A_{(1,2)n}^{TM,m_\nu} \cdot j \frac{\omega \varepsilon_0}{r \sin \vartheta} \cdot \frac{\sqrt{kr} \mathcal{Z}_{n+1/2}(kr)}{P_n^{m_\nu}(-\cos \vartheta_{1,2})} [P_n^{m_\nu}(-\cos \vartheta_{1,2}) \cdot P_n^{m_\nu}(\cos \vartheta) - P_n^{m_\nu}(\cos \vartheta_{1,2}) \cdot P_n^{m_\nu}(-\cos \vartheta)] \left(\frac{\cos}{\sin} \right) (m_\nu \varphi)'$$

$$H_{(1,2)\varphi} = -A_{(1,2)n}^{TM,m_\nu} \cdot j \frac{\omega \varepsilon_0}{r} \cdot \frac{\sqrt{kr} \mathcal{Z}_{n+1/2}(kr)}{P_n^{m_\nu}(-\cos \vartheta_{1,2})} [P_n^{m_\nu}(-\cos \vartheta_{1,2}) \cdot P_n^{m_\nu}(\cos \vartheta) - P_n^{m_\nu}(\cos \vartheta_{1,2}) \cdot P_n^{m_\nu}(-\cos \vartheta)] \frac{\cos}{\sin} (m_\nu \varphi)$$

$$\begin{aligned}
E_{(1,2)r} &= A_{(1,2)n}^{TM,m_\nu} \cdot \frac{kn(n+1)}{(kr)^2} \cdot \frac{\sqrt{kr} Z_{n+1/2}(kr)}{P_n^{m_\nu}(-\cos\vartheta_{1,2})} [P_n^{m_\nu}(-\cos\vartheta_{1,2}) \\
&\quad \cdot P_n^{m_\nu}(\cos\vartheta) - P_n^{m_\nu}(\cos\vartheta_{1,2}) \cdot P_n^{m_\nu}(-\cos\vartheta)] \frac{\cos}{\sin} \left\} (m_\nu\varphi) \\
E_{(1,2)\vartheta} &= A_{(1,2)n}^{TM,m_\nu} \cdot \frac{1}{kr} \cdot \frac{(\sqrt{kr} Z_{n+1/2}(kr))'}{P_n^{m_\nu}(-\cos\vartheta_{1,2})} [P_n^{m_\nu}(-\cos\vartheta_{1,2}) \\
&\quad \cdot P_n^{m_\nu}(\cos\vartheta) - P_n^{m_\nu}(\cos\vartheta_{1,2}) \cdot P_n^{m_\nu}(-\cos\vartheta)] \frac{\cos}{\sin} \left\} (m_\nu\varphi) \quad (A7) \\
E_{(1,2)\varphi} &= A_{(1,2)n}^{TM,m_\nu} \cdot \frac{1}{kr \sin\vartheta} \cdot \frac{(\sqrt{kr} Z_{n+1/2}(kr))'}{P_n^{m_\nu}(-\cos\vartheta_{1,2})} [P_n^{m_\nu}(-\cos\vartheta_{1,2}) \\
&\quad \cdot P_n^{m_\nu}(\cos\vartheta) - P_n^{m_\nu}(\cos\vartheta_{1,2}) \cdot P_n^{m_\nu}(-\cos\vartheta)] \left(\frac{\cos}{\sin} \right) \left\} (m_\nu\varphi) \right\}'
\end{aligned}$$

for TM-waves. The primes in equations (A6) and (A7) denote the derivative.

REFERENCES

1. Wilson, P. F., "Higher-order mode field distribution in asymmetric TEM cells," *URSI Int. Symp. on EM Theory*, Stockholm, Aug. 1989.
2. De Leo, R., et al., "Rigorous analysis of the GTEM cell," *IEEE Trans. on MTT*, Vol. MTT-39, No. 3, 488–500, March 1991.
3. Koch, M., "Analytische feldberechnung in TEM-Wellenleitern," Dissertation, Uni. Hannover, 1998.
4. Legendre, A. E., "Sur l'attraction des spheroides," *Mém. Math. Phys.*, 10, 1785.
5. Moon, P. and D. E. Spencer, *Field Theory Handbook*, Second edition, Springer-Verlag, Berlin, New York, 1971.
6. Pouhè, D., *Rechnerische und Messtechnische Untersuchung einer GTEM-Zelle*, Studienarbeit, TU Berlin, 1993.
7. Bronstein, I. N. and K. A. Semendjajew, *Taschenbuch der Mathematik*, 63, 23, Aufl., Verlag Harri Deutsch, 1987.
8. Piskounov, N., *Calcul Différentiel et Intégral*, Tomes 2, 92–95, 9^e édit., Édit. Mir, Moscou, 1980.
9. Hardy, G. H., *Divergent Series*, Chap. XIII, 320–321, Clarendon, 1949.
10. Pouhè, D., "Eine alternative Lösung der partikulären Legen-

dre'schen Wellengleichung $\frac{\partial^2 D(\vartheta)}{\partial \vartheta^2} + \cot \vartheta \cdot \frac{\partial D(\vartheta)}{\partial \vartheta} - \frac{m^2}{\sin^2 \vartheta} D(\vartheta) = 0$, private communication, TU Berlin, 1993.

11. Pouhè, D. and G. Mönich, "Geschlossene lösungen für den TEM-mode in GTEM-zellen," *Proc. Int. Kongress EMV 2000*, 277–286, Düsseldorf, February 2000.
12. Ramo, S., J. R. Whinnery, and T. van Duzer, *Fields and Waves in Communication Electronics*, 3rd edition, John Wiley & Sons, 1994.
13. Simonyi, K., *Theoretische Elektrotechnik*, 10. Auflage, Dt. Verlag der Wissenschaft, Leipzig, Berlin, Heidelberg, 1993.
14. Marcuvitz, N., *Waveguide Handbook*, 1st edition, New York, Toronto, London, 1951.
15. Pouhè, D., "On the theory of spherical waves in GTEM-cells: Higher-order modes in unloaded cells," *Proc. of IEEE Int. Symp. on EMC 2001*, Vol. 1, 408–43, Aug. 2001.
16. Kleinwachter, H., "Die Wellenausbreitung in zylindrischen Hohlleitern und die Hertz'sche Lösung als Sonderfälle der Wellenausbreitung in trichterförmigen Hohlleitern," *A.E.Ü.*, Band 5, S. 231–236, 1951.
17. Piefke, G., "Die Ausbreitung elektromagnetischer Wellen in einem Pyramiden-lichter," *Zeit. für ang. Physik*, VI. Band, Heft 11, S. 499–507, 1954.
18. Yamashita, E., *Analysis Methods for Electromagnetic Wave Problems*, Artech House, Boston, London, 1990.